

# Reconstruction and applications of consensus yeast metabolic network based on RNA sequencing

Yuqi Zhao<sup>1,\*</sup>, Yanjie Wang<sup>2,\*</sup>, Lei Zou<sup>3</sup> and Jingfei Huang<sup>1,4</sup>

1 State Key Laboratory of Genetic Resources and Evolution, Kunming Institute of Zoology, Chinese Academy of Sciences, Yunnan, China

2 Key Laboratory of Animal Models and Human Disease Mechanisms of Chinese Academy of Sciences and Yunnan Province, Kunming Institute of Zoology, Chinese Academy of Sciences, Yunnan, China

3 Department of General Surgery, First People's Hospital of Yunnan Province, Kunming, China

4 Collaborative Innovation Center for Natural Products and Biological Drugs of Yunnan, Kunming, Yunnan, China

## Keywords

metabolic engineering; metabolic network; RNA sequencing; *Saccharomyces* species

## Correspondence

Y. Zhao and J. Huang, State Key Laboratory of Genetic Resources and Evolution, Kunming Institute of Zoology, Chinese Academy of Sciences, No. 32 Jiaochang Donglu, Kunming 650223 Yunnan, China  
Fax/Tel: 86-0871-5199200  
E-mails: zhaoyq@mail.kiz.ac.cn; huangjf@mail.kiz.ac.cn

\*These authors contribute equally to the study.

(Received 12 November 2015, revised 8 January 2016, accepted 13 January 2016)

doi:10.1002/2211-5463.12033

One practical application of genome-scale metabolic reconstructions is to interrogate multispecies relationships. Here, we report a consensus metabolic model in four yeast species (*Saccharomyces cerevisiae*, *S. paradoxus*, *S. mikatae*, and *S. bayanus*) by integrating metabolic network simulations with RNA sequencing (RNA-seq) datasets. We generated high-resolution transcriptome maps of four yeast species through *de novo* assembly and genome-guided approaches. The transcriptomes were annotated and applied to build the consensus metabolic network, which was verified using independent RNA-seq experiments. The expression profiles reveal that the genes involved in amino acid and lipid metabolism are highly coexpressed. The diverse phenotypic characteristics, such as cellular growth and gene deletions, can be simulated using the metabolic model. We also explored the applications of the consensus model in metabolic engineering using yeast-specific reactions and biofuel production as examples. Similar strategies will benefit communities studying genome-scale metabolic networks of other organisms.

The metabolic network reconstructions can be applied in diverse aspects, such as metabolic engineering for biotechnological productions [1], and interrogation of multispecies relationships [2]. Among these applications, the cross-species comparison of metabolic networks allow for a systematic investigation of structure-function relationships of biological processes and may put forth valuable hints on the evolution of these metabolic pathways [3–5]. For instance, the consequences of copy number alterations in metabolic networks suggested a potential role for dosage

selection in the mammalian evolution [3]. In addition, a ‘community consensus’ reconstruction of the yeast metabolic network was performed by Herrgård *et al.* [6], which was based on a large, focused work meeting, to define the protocol for the curation process as well as resolving the majority of discrepancies between the existing reconstructions.

However, the majority of the current metabolic networks are reconstructed based on the prior knowledge (knowledge-driven) and focused on network topologies or characteristics of components in the

## Abbreviations

DEG, Differentially Expressed Genes; FBA, Flux Balance Analysis; GDLS, Genetic Design through Local Search; IMOMA, Linear Minimization Of Metabolic Adjustment; MOMA, Minimization Of Metabolic Adjustment; PCC, Pearson's correlation coefficient; PYRDC, Pyruvate decarboxylase; RPKM, Reads Per Kilobase of exon per Million reads.

model, ignoring the actual states of the metabolic networks [7]. For instance, the transcriptomes in cells should always be considered, in which the changes are critical for generating phenotypic diversity among species [8]. On the other hand, the gene expression divergence may lead to the failures of repeating biological experiments or of developing medicines in scientific research field [8]. Recent advances in sequencing technology have made it available to derive accurate metabolic models [9,10]. In theory, RNA-seq can be applied to reconstruct complete and high-resolution transcriptomes across all species, cell types and states [11–13]. Several methods have been developed to build the transcriptome, and they fall into two main classes: ‘genome-guided’ and genome-independent (*de novo* assembly) [14]. The first methods rely on a reference genome to first map all the RNA-seq reads to the genome and then assemble overlapping reads into transcripts. Unfortunately, the genome-guided method does not always work. Despite the large drop in the cost of next-generation sequencing, the complete study of a genome is still costly and difficult, especially for nonmodel organisms. Besides, the model being studied is sufficiently different from the reference genome because it comes from a different strain or line. In this situation, *de novo* assembly is suitable for the accurate reconstructions.

In the study, we carried out an integration analysis of RNA-seq expression profiles from four yeast species (*Saccharomyces cerevisiae*, *Saccharomyces paradoxus*, *Saccharomyces mikatae*, and *Saccharomyces bayanus*) to generate a ‘consensus’ metabolic network. First, we generated high-resolution transcriptome maps of four yeast species through *de novo* assembly and genome-guided approach. We then produced a consensus metabolic network and validated the model using an independent RNA-seq study. By quantifying the gene expression level in the model, we estimated the conservation and divergence of metabolic pathways. We also discussed the practical applications of the metabolic model.

## Materials and methods

### Overview

The process, explained in detail below and illustrated in Fig. 1, consists of four steps: (a) genome-guided transcriptome reconstruction; (b) *de novo* transcriptome assembly; (c) reconstruction of consensus metabolic model; and (d) model annotations, simulations, and validation.

### RNA-Seq data acquisition and metabolic network of *Saccharomyces cerevisiae*

The raw RNA-seq data from four yeast species (*S. cerevisiae*, *S. paradoxus*, *S. mikatae*, and *S. bayanus*) was downloaded from the NCBI GEO database (NCBI GEO accession: GSE32679) [15], with two replicates for each species. The four yeast species were grown in complete media and sampled according to the protocol described in Marth *et al.*'s study [15].

The *S. cerevisiae* iND750 metabolic network (hereinafter referred to as ‘iND750’) was retrieved from Schellenberger *et al.*'s work [16]. It contains 1061 metabolites, which participate in 1266 reactions in 47 subsystems, catalyzed by 750 verified *S. cerevisiae* genes. The model is available as a systems biology markup language (SBML) [17] file, which could be easily used in the MATLAB-compatible COBRA Toolbox [18].

### Genome-guided transcriptome reconstruction

The reference genome and annotations for *S. cerevisiae* were obtained from the Saccharomyces Genome Database (<http://www.yeastgenome.org/>). Genome, annotations, and orthology mappings for the other species were from Kellis *et al.*'s work [19]. RNA-seq reads were aligned to their respective genomes using the MOSAIK alignment program (version 1.1.0018, <http://bioinformatics.bc.edu/marthlab/Mosaik>) allowing for a threshold of two mismatches between each 35-base pair read and the reference genome. The alignment output was parsed using the bamtools API [20].

### *De novo* transcriptome assembly

All the *de novo* assemblies were run with OASES (version 0.2.08) [21], and VELVET (version 1.2.07) [22]. In each of the assemblies, the RNA-seq reads were used to build a de Bruijn graph through Velvet, with the k-mer lengths of 17, 19, 21, 23, 25, 27, 29, 31, and 33, respectively. The Bruijn graphs were then simplified for errors, organized into a scaffold, divided into loci, and finally analyzed to extract transcript assemblies or transfrags. Once all of the individual k-mer assemblies were finished, they were merged into a final assembly.

### Reconstruction of consensus metabolic model

In the process, the BLASTN (version 2.2.23) program was used to map all the metabolic genes in *S. cerevisiae* model to the transcriptomes reconstructed through genome-guided approach and *de novo* assembly, with e-value threshold set at  $10^{-4}$ . We then overlapped all the positive results from four species to obtain a consensus metabolic gene dataset.

We derived a consensus metabolic model from the *S. cerevisiae* metabolic network using two commonly used

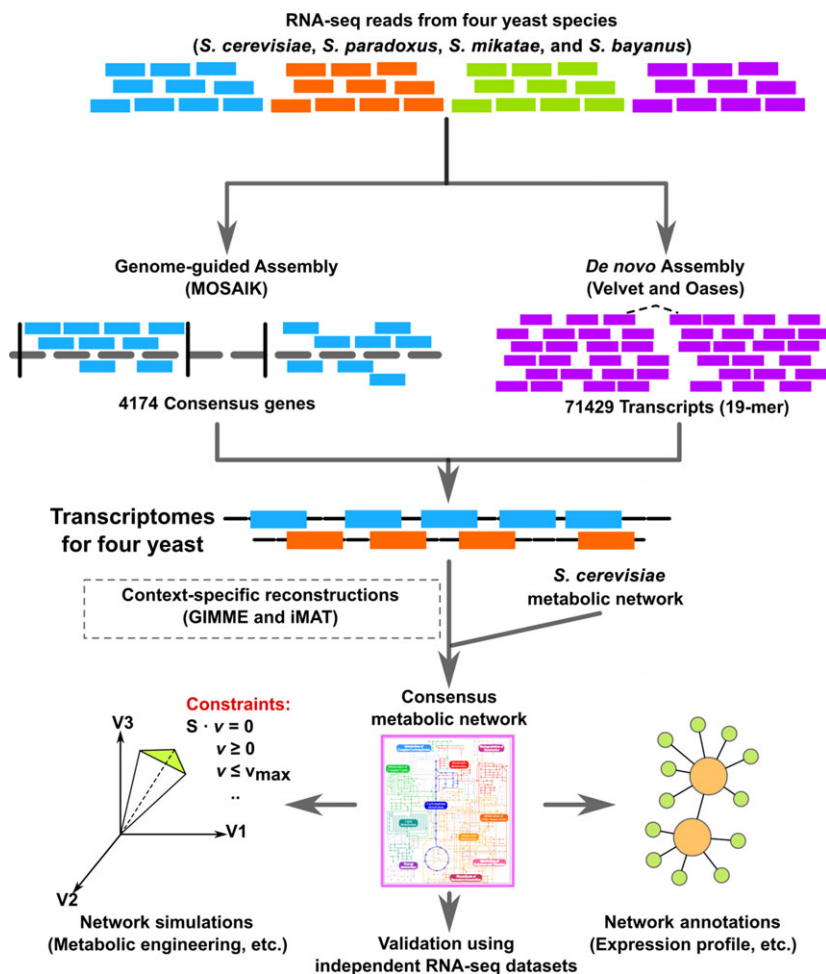


**Fig. 1.** A flowchart schematic representation of our study. The process consists of four steps: (1) genome-guided transcriptome reconstruction; (2) *de novo* transcriptome assembly; (3) reconstruction of consensus metabolic model; and (4) model validation, simulation, and annotation. In step (4), we determined the conservation and divergence of metabolic genes in gene expression.

algorithms of top-down metabolic reconstructions, including GIMME [7] and iMAT [23]. The GIMME algorithm is a linear programming procedure, which can match high-throughput omics data (such as transcriptome and proteome) to an original flux distribution that obtained from the full metabolic model. The constraining reactions in the consensus were set up according to the Yeast 5 genome-scale model [24]. On the other hand, the iMAT algorithm is a mixed integer linear programming algorithm that best matches the omics data to pathway length. Using these two methods for the consensus model reconstruction, (a) we prepared the *S. cerevisiae* metabolic network, and (b) the high-quality transcriptomes in four species based on the genome-guided and *de novo* methods above.

### Differential expression in pairwise comparison

We identified differentially expressed genes (DEGs) using a free BIOCONDUCTOR [25] package, called DESEQ (version 1.1.11) [26]. In RNA-seq experiments, read counts differ

for each sample due to a variable number of reads produced by sequencing runs and the mixture of RNA within samples. Sample normalization is confounded by differences in gene expression. To solve the problem, DESeq uses a generalization of the Poisson model, the negative binomial distribution, to model biological and technical variance and test for differential expression between the two conditions or species. All genes that were found to be DEGs between two species (at a *P*-value cutoff of 0.05 and fold-change  $< 0.5$  or  $> 2$ , that is, fold-change  $< -1$  or  $> 1$  after log transformation) were retained for further analysis. We also applied reads per KB per million reads (RPKM) to detect gene expression levels [27].

To reduce the bias induced by randomization, we introduced the phastCons tree model [28] with branch lengths for all four species (Fig. S1), with *S. bayanus* included in the further analysis as an outgroup. If a DEG between *S. bayanus* and the other three species show the same tendency (i.e., all the fold changes  $> 2$  or  $< 0.5$ ), the gene was considered to form divergent expression patterns.

## Validation of the metabolic model using independent RNA-seq study

To validate our metabolic model, we introduced another independent RNA-seq dataset (NCBI GEO accession: GSE38875), with two replicates for *S. paradoxus*, *S. mikatae*, and *S. bayanus*, and six replicates for *S. cerevisiae* [29]. Cultures were grown at 25 °C in yeast extract peptone dextrose medium to log phase. The RNA-seq reads were analyzed using the same procedures in Fig. 1: (a) the transcriptomes for the four yeast species were reconstructed using both genome-guided and *De Novo* assembly methods, and (b) the consensus metabolic model was built using GIMME [7] and iMAT [23] algorithms based on the reconstructed transcriptomes and *S. cerevisiae* iND750 [16]. Moreover, we compared our metabolic network with manually curated metabolic networks, including YEAST5 [30] and YEAST6 [31].

## Reconstruction of coexpression network

We combined the two independent RNA-seq datasets together, and got 20 expression profiles in total for the four yeast species. The genes were ranked according to expression variance among samples and the ones with lowest variance (the top 25 percentile) were filtered. We then adopted the Pearson's correlation coefficient (PCCs) of gene expression patterns to measure the gene coexpression. To make the result solid, we set  $|\text{Pearson's } r| > 0.90$ .

## Metabolic network simulations

The metabolic models were analyzed by using multiple methods in COBRA toolbox (V 2.0.2) [18], including flux balance analysis (FBA) [32], minimization of metabolic adjustment (MOMA) [33], and Genetic Design through Local Search (GDLS) [34].

These methods provide important tools for harnessing the knowledge encoded in the reconstructed metabolic model. FBA predicts metabolic flux distributions at steady state by using linear programming while the method of minimization of metabolic adjustment (MOMA) employs quadratic programming to identify a point in flux space, which is closest to the wild-type point, compatibly with the gene deletion constraint. FBA and MOMA of the metabolic network were used to calculate the impact of gene deletions on maximum biomass production rate (a proxy for fitness). We set both the upper and lower flux bounds of the reaction(s) involving the deleted gene to zero. The gene-reaction associations in the model are indicated by logical relationships between metabolic genes and their corresponding reactions. That is, if a single gene participates in multiple reactions, the gene deletion will result in the removal of all associated reactions. On the other hand, if a reaction involves multiple noninteracting genes, it will

not be silenced in a single gene deletion. We categorized the simulation results from a single gene deletion into non-lethal and lethal, which correspond to unchanged maximal growth (defined as mutant growing at > 99.9% of the wild-type growth rate) and reduced maximal growth or no growth separately. We can obtain valuable information by exploring the effect of reducing flux through a single reaction on growth, for example, predicting the haploinsufficient phenotypes in yeasts. Moreover, robustness analysis of the metabolic network tells us how growth rate changes as the flux through a specific reaction of interest varies in magnitude [35].

The GDLS algorithm [34] was used to identify the reactions list to knock out in order to increase *in silico* production of desired metabolites. GDLS is a computational design tool for metabolic engineering, which uses an efficient, low-complexity local search approach to identify favorable genetic designs from flux balance metabolic models [34]. In this study, we set neighborhood size to be 2, maximum number of knockouts to be 5, and the minimum growth rate to be  $0.05 \text{ mmol gDW}^{-1} \text{ h}^{-1}$  [36]. The model was adjusted as the minimal medium composition to be aerobic and contain a glucose supply ( $20 \text{ mmol gDW}^{-1} \text{ h}^{-1}$ ).

## Essential genes in yeast genome

We retrieved the essential genes for yeast growth from *Saccharomyces* Genome Deletion Project ([http://www-sequence.stanford.edu/group/yeast\\_deletion\\_project](http://www-sequence.stanford.edu/group/yeast_deletion_project)), which generates more than 20000 strains with the overall goal of assigning function to the ORFs through phenotypic analysis of the mutants [37]. Based on the gene deletion experiments, the single gene deletion results using FBA and IMOMA can be categorized into: True Positives (model simulation predicts growth when inessential genes are deleted), False Negatives (model simulation predicts no growth when inessential genes are deleted), False Positives (model simulation predicts growth when essential genes are deleted), and True Negatives (model simulation predicts no growth when essential genes are deleted).

## Gene ontology and statistical analysis

All the Gene Ontology enrichment analyses were assessed using ClueGO, a Gene Ontology-based tool as functionally grouped networks [38]. KEGG pathway analysis was also performed using ClueGO. Two-sided hypergeometric test was adopted as the default statistical test. Tukey–Kramer test was performed to determine the statistical significance of the average length of assembled transcripts from different k-mers. Two-sample *t*-test was performed to compare the gene expression levels between metabolic genes.

## Results

### Integrated analysis of genome-guided and *de novo* assembly

We searched transcripts of each species obtained through the genome-guided method against the sequences from the other three species and retrieved 4174 consensus transcripts (Fig. 2A), accounting 78.7% of the annotated cDNA sequences in *S. cerevisiae*. Of these consensus genes, 545 were found to be metabolic genes in *S. cerevisiae* metabolic genes. Meanwhile, molecular function enrichment analysis with Gene Ontology annotation reveals that the transcripts not included in consensus dataset from *S. cerevisiae* are

enriched with DNA-binding (GO:00036770), protein kinase activity (GO:00046720), and transcription factor binding (GO:00081340) and other important function categories (the detailed information was depicted in Fig. S2; all  $P$  values  $< 0.01$ ), which are crucial for cell growth. KEGG pathway analysis shows that the metabolic genes not included in the consensus dataset were enriched with basic metabolic pathways (Fig. 2B), such as Glutathione metabolism (KEGG:004800), and Glycolysis/Gluconeogenesis (KEGG:000100).

We reasoned that there were missing consensus genes between four yeast species due to the incomplete genome information. As a result, we carried out *de novo* assembly of  $2.9 \times 10^8$  RNA-seq reads to generate a high-resolution transcriptome map. In the

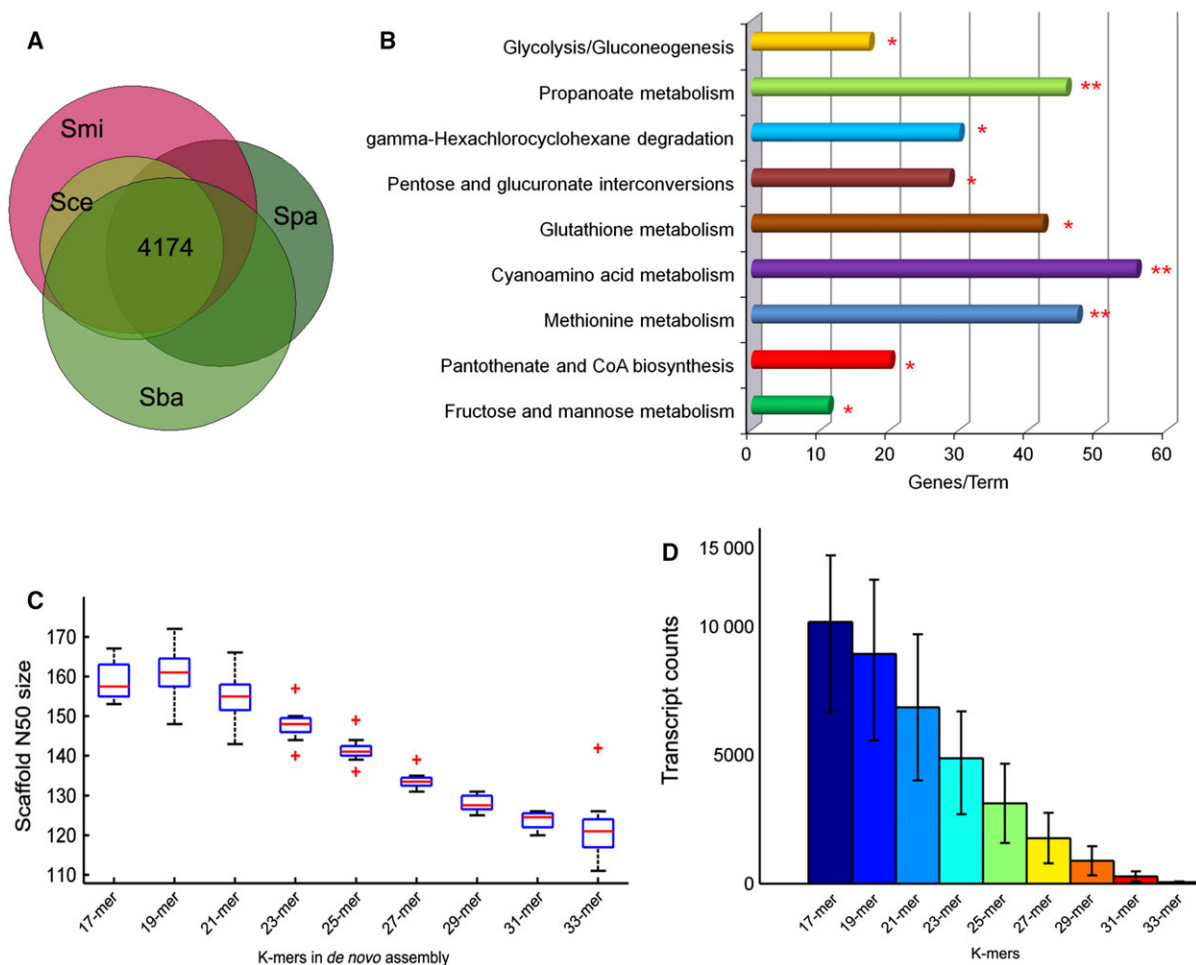


**Fig. 2.** Transcriptome assembly using RNA-seq reads. (A) Venn plot of transcripts of four yeast species obtained through the genome-guided method, with 4174 consensus transcripts. Sce, Spa, Smi, and Sba represent *Saccharomyces cerevisiae*, *S. paradoxus*, *S. mikatae*, and *S. bayanus* separately. (B) KEGG pathway analysis of the metabolic genes not included in the consensus enzymes obtained through the genome-guided method. The red stars indicate statistical significance (two stars when  $P < 0.01$ ; one star when  $P < 0.05$ ). (C) The scaffold N50 values when the k-mer was set to 17, 19, 21, 23, 25, 27, 29, 31, and 33 in *de novo* assembly. (D) The average transcript count in each species when the k-mer was set to 17, 19, 21, 23, 25, 27, 29, 31, and 33 in *de novo* assembly.

single k-mer assembly in oases and velvet protocol, the average length of scaffolds was highest when the k-mer was set to 19 (Fig. 2C; Tukey–Kramer test,  $P = 5.7 \times 10^{-7}$ ). Besides, the transcripts retrieved from 19-mer performed best in the following BLAST analysis, which were therefore used for the further analysis. Oases assembles 71429 transcripts in four yeast species, with two replicates in each species merged into one transcriptome (Fig. 2D). In these transcripts, we detected 217 consensus metabolic genes included in *S. cerevisiae* model. We combined transcriptomes from genome-guided and *de novo* assembly strategies and obtained 599 consensus metabolic genes in four yeast species.

### Reconstruction and validation of consensus metabolic network in four yeast species

Based on iND750 and the transcriptomes above, we applied two common methods (Materials and Methods) to reconstruct a consensus metabolic network. It shows that the two methods produced the equivalent network, containing 992 metabolites, which participate in 1104 reactions, catalyzed by 604 metabolic genes (TEXT S1). The model was written in systems biology markup language and could be divided into 47 subsystems (Fig. S3). It is observed that different gene-protein-reaction (GPR) relationships are adopted in different subsystems. For example, reactions in oxidative phosphorylation are often catalyzed by multiple genes while genes in fatty acid biosynthesis correspond to multiple reactions.

Using an independent RNA-seq dataset [29], we repeated the procedure for model reconstruction with all the parameters the same (Materials and Methods). The reconstructed transcriptomes contains 4728 consensus transcripts from genome-guided assembly approach and 73 661 transcripts from *de novo* assembly approach. A total of 602 consensus metabolic genes were found from the transcriptomes. A metabolic model containing 992 metabolites, 1104 reactions, and 604 metabolic genes was obtained. It shows that the model contains the same GPR relationships as the one in TEXT S1, suggesting that the reconstructed model is robust. Moreover, compared to the manually curated metabolic networks [30,31], the data-driven network reconstruction we adopted is stable among different datasets. For example, YEAST6 comprises 1458 metabolites participating in 1888 reactions, which are annotated with 900 yeast genes encoding the catalyzing enzymes [31]. Meanwhile, YEAST5 includes 1655 metabolites participating in 2110 reactions [30]. Another advantage of the

data-driven strategy is the ease to add additional inputs to the metabolic model. For instance, it would be necessary to consider the actual states (gene expression, DNA methylation, etc.) of the metabolic network.

### Expression patterns of metabolic genes

Gene expression is a sensitive measure to observe the molecular change [8]. It is commonly accepted that highly expressed genes tend to be essential and evolve at lower rates [39]. As a result, we first explored the highly expressed metabolic genes in the yeast consensus metabolic model. Figure 3 shows the top 40 highly expressed metabolic genes in *S. bayanus*, most of which show high expression in other three species. By setting stringent criteria (all fold change  $\geq 2$  or  $\leq 0.5$ , and  $P < 0.05$  between *S. bayanus* and the other three species), we identified seven genes divergent in gene expression. Among these seven genes, gene FAS2 (Fatty acid synthase subunit alpha) shows up-regulated patterns while the other six genes (ACO1, PCM1, IPP1, MET5, MES1, and TPS1) show down-regulated patterns between *S. bayanus* and the other three species. It shows that the protein encoded by *S. bayanus* FAS2 is much longer than the orthologous proteins in the other species, with large deletions/insertions in the multiple sequence alignment. We also detected FAS2 with positive selection on coding region ( $P < 10^{-5}$ ), using the Nei–Gojobori method [40] and the bootstrap method (500 replicates) in MEGA5 [41].

We also wondered whether the metabolic genes in the model displayed the same patterns in expression profiles with each other. As a result, we built up a coexpression network based on the intra- and inter-species expression variation (Fig. 4; Methods). It shows that most of the coexpressed genes are associated with amino acid and lipid metabolism. Besides, 10 metabolic genes present a densely connected module, mainly participating in Glycolysis/Gluconeogenesis and Phospholipid Biosynthesis.

### Simulating phenotypic characteristics of metabolic model

Using the metabolic model, we could predict phenotypes of yeast metabolic genes. In the previous studies, one of the most important phenotypic predictions is the simulation of cellular growth [35]. As a result, we defined biomass composition of the cell as the biomass objective function and performed FBA on the reconstructed network to maximize the objective function. It

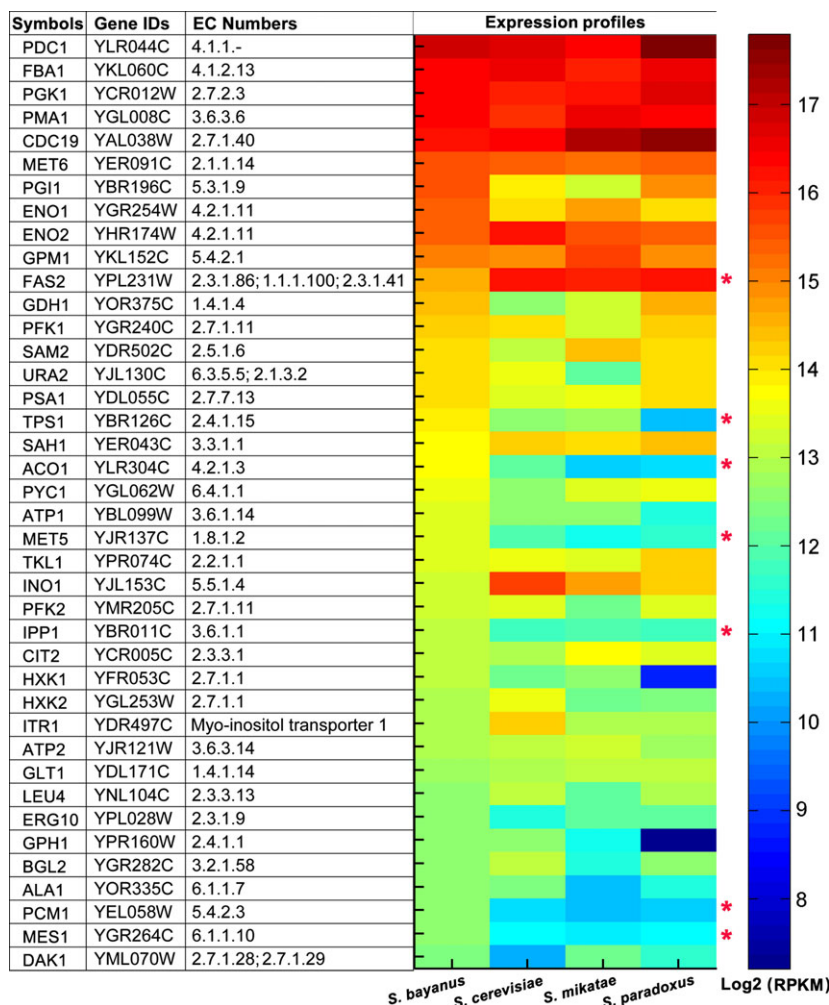


**Fig. 3.** The expression patterns of highly expressed *Saccharomyces bayanus* metabolic genes in four yeast species. The heat map shows the log<sub>2</sub> transform of RPKM (reads per kilobase of exon per million reads) values of metabolic genes in the consensus metabolic model. Red stars indicate differentially expressed genes with the changes in RPKM ratio over twofold and  $P < 0.01$  between *S. bayanus* and the other three species.

shows that the optimal solution for the model is the same as the optimal solution in *S. cerevisiae* metabolic network (optimal flux = 0.097).

We performed a genome-scale single gene deletion study using both FBA and linearMOMA methods in COBRA toolbox [35]. It shows that 113 genes were considered lethal and 491 genes were nonlethal out of 604 genes in the model, with 95 gene deletions leading to reduced maximal growth rates and 396 exhibiting no change in growth using FBA (Fig. S4A). The growth ratios of 331 gene deletions to wild-type are different between two methods. It is mainly due to the different flux-based analysis strategies by FBA and IMOMA [33]. Compared with FBA, IMOMA is based on the same stoichiometric constraints, but the optimal growth flux for mutants is relaxed, providing an approximate solution for a suboptimal growth flux state. However, it shows that the lethal genes predicted using FBA are also predicted lethal using IMOMA, suggesting that prediction of essential metabolic genes

from both methods are consistent. In addition, the single gene deletion results show that biomass could be produced in 451 out of 492 the gene-deletion strains in which genes annotated as inessential or nonauxotrophic were deleted (true positive) and that biomass could not be produced in 48 mutant strains where these inessential or nonauxotrophic genes were deleted (false negative). As a result, the consensus metabolic model has a 90.4% sensitivity for identifying the essential genes. If the simulation results predicted that biomass could be produced following a gene deletion, the deleted gene was not considered as essential in 92% of the cases (a 92% positive predictive value).

We wondered the effects of reducing flux through reactions catalyzed by the highly expressed genes in consensus metabolic model. As a result, we studied the effect of decreasing the expression level of the top two genes (Fig. S4B) on the growth rate to predict haploinsufficient phenotypes. The gene YLR044C (pyruvate decarboxylase; EC 4.1.1) participates in Pyruvate

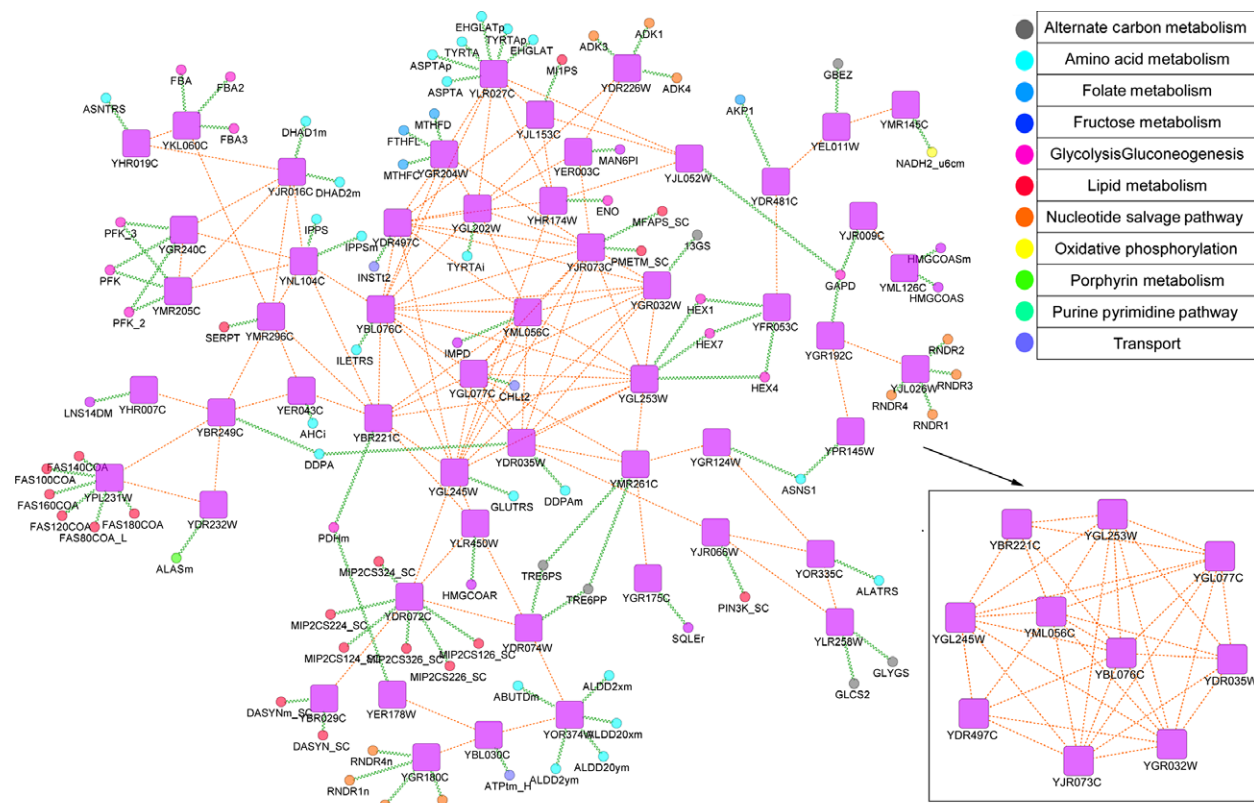


**Fig. 4.** Coexpression network of metabolic genes based on the intra- and interspecies variation in gene expression. Only the main island of the coexpression network is shown. gra: gene-reaction association; pp: coexpression relationships between metabolic genes.

Metabolism while the gene YKL060C (fructose-bisphosphate aldolase; EC 4.1.2.13) catalyzed Glycolysis/Gluconeogenesis. The growth rate is sustained near the optimal value over a range of fluxes for Pyruvate Metabolism (PYRDC, Pyruvate decarboxylase) while the growth rate for Glycolysis/Gluconeogenesis (fructose-bisphosphate aldolase) is sharply reduced after optimal value, indicating network robustness with respect to flux changes in PYRDC (Fig. S4B). However, a complete deletion of the PYRDC reaction would lead to a lethal phenotype, whereas deletion of the fructose-bisphosphate aldolase reaction exhibits no change in growth.

### Applications of consensus model in metabolic engineering

One important use of metabolic reconstructions is to guide of metabolic engineering in yeast [42], for example, overproduction of biofuels [43]. Here, we applied the model to identify how to increase *in silico* production of desired metabolites. We took yeast-specific reactions and ethanol as examples.

We searched the Yeast Metabolome Database (<http://www.ymdb.ca/>) using metabolic genes in the metabolic model and identified 54 yeast-specific reactions (Table S1). We set the minimal medium composition of the metabolic model aerobic and contain a glucose supply ( $20 \text{ mmol gDW}^{-1} \text{ h}^{-1}$ ) and predicted a list of candidate reactions for deletion to optimize product formation of these yeast-specific reactions (Table 1). It shows that seven out of the 54 reactions can be optimized by reaction knockouts. Besides, it also shows that 2-oxoglutarate exchange (EX\_aki) can be knocked out for the overproduction of five specific reactions.

We estimated the *in silico* overproduction of ethanol, zymosterol, and D-sorbitol as biofuel production. The resulting knockout list for ethanol is aldehyde dehydrogenase acetaldehyde NADP, catalase, CO<sub>2</sub> transport diffusion mitochondrial, glucose 6 phosphate isomerase, and threonine aldolase (Table 2). The resulting knockout predicted a growth rate of  $\sim 0.21$  and a product excretion rate of  $\sim 37.29$ . As for zymosterol, the resulting knockout predicted a growth rate of  $\sim 0.44$  while a product excretion rate of  $\sim 1.50$ . We set the maximum number of knockouts to be no limit, the list of reactions



to knock out increases to 12 (the list for zymosterol in Table 2 plus ALATA\_L, BPNT, GHMT2r, GLYt2 m, HSK, IPPS, NDPK1). However, the growth rate is reduced  $\sim 0.28$  and the production rate increases to  $\sim 1.67$ . For D-Sorbitol, The optimal knockouts are transketolase, L-alanine transaminase, 3-5-bisphosphate nucleotidase, ergosterol exchange, and h2o transport via diffusion. Both ethanol and D-Sorbitol result in the some similar optimal flux distribution.

## Discussion

In the recent 10 years, network reconstruction approaches have developed rapidly [7,44]. The yeast metabolic reconstruction presented here represents an analogous process for systems biology studies of a target organism. With the successful achievement of the consensus reconstruction based on RNA-seq, similar strategies should benefit systems biology for other organisms in metabolic modeling. We believe that the metabolic model reconstruction provided here will have special utility in a number of areas. First, the reconstruction will allow successful phenotype predictions, including cell growth, in response to genetic and/or environmental perturbations using a variety of methods [6]. In the study, we simulated gene deletion phenotypes and robustness analysis of specific reactions. The results are of importance to studying molecular functions of metabolic genes. Second, we can perform an exploration of metabolic pathways and well-curated connections between gene products. With the inevitable depletion of the world's energy supply, there has been an urgent need in alternative sources of energy. In the recent years, many scientists are increasingly conscious of biomass energy as a means of providing modern energy [45]. The results show that we can apply the consensus metabolic model in biofuel production. Moreover, we can optimize the overproduction of specific metabolites (such as ethanol) through gene knockouts. Third, it can be integrated

**Table 2.** Metabolic engineering of consensus metabolic model for biofuel production.

	Ethanol	Zymosterol	D-Sorbitol
Knockout list	ALDD2y, CAT, CO2tm, PGI, THRA	CSNAT, ERGSTt, ME1 m, PYRt2 m, TKT2	ALATA_L, BPNT, EX_ergst(e), H2Ot, TKT2
Product	37.29	1.50	14.2
Biomass	0.21	0.44	0.12

The concentration of product and biomass is mmol gDW<sup>-1</sup> h<sup>-1</sup>. ALDD2y: aldehyde dehydrogenase acetaldehyde NADP; CAT: catalase; CO2tm: CO2 transport diffusion mitochondrial; PGI: glucose 6 phosphate isomerase; THRA: Threonine aldolase; CSNAT: carnitine O acetyltransferase; ERGSTt: ergosterol reversible transport; ME1 m: malic enzyme NAD mitochondrial; PYRt2 m: pyruvate mitochondrial transport via proton symport; TKT2: transketolase; ALATA\_L: L-alanine transaminase; BPNT: 3-5-bisphosphate nucleotidase; EX\_ergst(e): Ergosterol exchange; H2Ot: H2O transport via diffusion.

with other high-throughput data, such as microarray [46], genomic information [47], and proteomics [48], for exploring questions related to comparative metabolomics and of metabolic pathway evolution.

Yeasts can cause a spectrum of diseases that range from colonization to uniformly fatal invasive disease. For example, Invasive fungal diseases (IFDs) are increasingly common complications in critically ill patients worldwide and are frequently fatal [49]. Referring to yeast biology, several groups have stressed the threat that the lack of new antifungal drugs of broad spectrum and low toxicity poses to public health [50]. We reason that the yeast metabolic model is suitable for drug development. There are several available strategies for this. First, the structures of 100 metabolic proteins have been solved to date, which can be easily applied in the drug design [51]. Second, the systems biology tools, especially the constraint-based modeling of genome-scale metabolic networks, can be used in exploring pathogenic processes and drug discovery [52]. In addition, we explored the conservation and divergence of the

**Table 1.** Metabolic engineering of yeast-specific reactions using *in silico* GDLS optimizations.

	MFAPS	PETOHM	PINOS	PMETM	PSERDv	DAGPYP	PStv
Knockouts	EX_akg	EX_akg	EX_akg, HMGCOAtm	EX_akg	PStm	EX_akg, HMGCOAtm	PStm
Product	0.012	0.012	0.01	0.012	0.02	0.013	$2.0 \times 10^{-4}$
Biomass	1.95	1.95	1.95	1.95	1.95	1.95	1.95

The concentration of product and biomass is mmol gDW<sup>-1</sup> h<sup>-1</sup>. EX\_akg: 2 Oxoglutarate exchange; HMGCOAtm: Hydroxymethylglutaryl CoA reversible mitochondrial transport; PStm: phosphatidylserine mitochondrial transport; MFAPS: methylene fatty acyl phospholipid synthase; PTOHM: phosphatidylethanolamine N methyltransferase; PINOS: phosphatidylinositol synthase; PMETM: Phosphatidyl N methylethanolamine N methyltransferase; PSERDv: phosphatidylserine decarboxylase; DAGPYP: diacylglycerol pyrophosphate phosphatase; PStv: phosphatidylserine vacuolar transport.

metabolic genes in gene expression. The majority of the consensus metabolic genes is conserved, which can provide useful evolutionary information for targets of broad-spectrum therapeutics.

Despite our experimental and statistical rigor, our dataset does have some limitations. We used two RNA-seq datasets with 20 samples to reconstruct the coexpression network, which may not cover the entire temporal differentially expressed genes. Besides, the reconstructed metabolic model is not robust to the changing flux through a single reaction. Some of the links between reactions or nodes (including metabolites, reactions, or genes) might be missing. The future work should focus on the filling gaps in metabolic pathways.

## Conclusion

In this study, we reconstructed a consensus metabolic model in four yeast species based on RNA-Seq datasets. The metabolic model can be applied to metabolic engineering and benefit communities studying genome-scale metabolic networks of other organisms.

## Acknowledgement

This work was supported by the grants from National Natural Science Foundation of China (Grant No. 81400084; Grant No. 31123005), National Basic Research Program of China (2013CB835100).

## Author contributions

YZ, YW carried out the RNA-seq data analysis, network simulations, and drafted the manuscript. LZ performed all the statistical analysis, and helped draft the paper. JH conceived of the study, and helped to draft the manuscript. All authors read and approved the final manuscript.

## References

- Oldiges M, Eikmanns BJ and Blombach B (2014) Application of metabolic engineering for the biotechnological production of L-valine. *Appl Microbiol Biotechnol* **98**, 5859–5870.
- Oberhardt MA, Palsson BO and Papin JA (2009) Applications of genome-scale metabolic reconstructions. *Mol Syst Biol* **5**, 320.
- Bekaert M and Conant GC (2011) Copy number alterations among mammalian enzymes cluster in the metabolic network. *Mol Biol Evol* **28**, 1111–1121.
- Flynn RL, Centore RC, O'Sullivan RJ, Rai R, Tse A, Zhou SY, Chang S, Karlseder J and Zou L (2011) TERRA and hnRNPA1 orchestrate an RPA-to-POT1 switch on telomeric single-stranded DNA. *Nature* **471**, 532.
- Mintz-Oron S, Meir S, Malitsky S, Ruppin E, Aharoni A and Shlomi T (2012) Reconstruction of *Arabidopsis* metabolic network models accounting for subcellular compartmentalization and tissue-specificity. *Proc Natl Acad Sci USA* **109**, 339–344.
- Herrgard MJ, Swainston N, Dobson P, Dunn WB, Arga KY, Arvas M, Bluthgen N, Borger S, Costenoble R, Heinemann M *et al.* (2008) A consensus yeast metabolic network reconstruction obtained from a community approach to systems biology. *Nat Biotechnol* **26**, 1155–1160.
- Becker SA and Palsson BO (2008) Context-specific metabolic networks are consistent with experiments. *PLoS Comput Biol* **4**, e1000082.
- Zhao YQ, Sheng ZZ and Huang JF (2012) A systematic analysis of heart transcriptome highlights divergent cardiovascular disease pathways between animal models and humans. *Mol BioSyst* **8**, 504–510.
- Varemo L, Scheele C, Broholm C, Mardinoglu A, Kampf C, Asplund A, Nookaew I, Uhlen M, Pedersen BK and Nielsen J (2015) Proteome- and transcriptome-driven reconstruction of the human myocyte metabolic network and its use for identification of markers for diabetes. *Cell Rep* **11**, 921–933.
- Solomon KV, Haitjema CH, Thompson DA and O'Malley MA (2014) Extracting data from the muck: deriving biological insight from complex microbial communities and non-model organisms with next generation sequencing. *Curr Opin Biotech* **28**, 103–110.
- Zhao Y-Q, Li G-H and Huang J-F (2013) Comparative systems biology between human and animal models based on next-generation sequencing methods. *Zool Res* **34**, 35–41.
- Zhao Y, Ji S, Wang J, Huang J and Zheng P (2014) mRNA-Seq and MicroRNA-Seq whole-transcriptome analyses of rhesus monkey embryonic stem cell neural differentiation revealed the potential regulators of rosette neural stem cells. *DNA Res* **21**, 541–554.
- Zhao Y, Barrere-Cain RE and Yang X (2015) Nutritional systems biology of type 2 diabetes. *Genes & Nutrition* **10**, 481.
- Garber M, Grabherr MG, Guttman M and Trapnell C (2011) Computational methods for transcriptome annotation and quantification using RNA-seq. *Nat Methods* **8**, 469–477.
- Busby MA, Gray JM, Costa AM, Stewart C, Stromberg MP, Barnett D, Chuang JH, Springer M and Marth GT (2011) Expression divergence measured by transcriptome sequencing of four yeast species. *BMC Genom* **12**, 635.

- 16 Schellenberger J, Park JO, Conrad TM and Palsson BO (2010) BiGG: a Biochemical Genetic and Genomic knowledgebase of large scale metabolic reconstructions. *BMC Bioinformatics* **11**, 213.
- 17 Hucka M, Finney A, Sauro HM, Bolouri H, Doyle JC, Kitano H, Arkin AP, Bornstein BJ, Bray D, Cornish-Bowden A *et al.* (2003) The systems biology markup language (SBML): a medium for representation and exchange of biochemical network models. *Bioinformatics* **19**, 524–531.
- 18 Schellenberger J, Que R, Fleming RMT, Thiele I, Orth JD, Feist AM, Zielinski DC, Bordbar A, Lewis NE, Rahmanian S *et al.* (2011) Quantitative prediction of cellular metabolism with constraint-based models: the COBRA Toolbox v2.0. *Nat Protoc* **6**, 1290–1307.
- 19 Kellis M, Patterson N, Endrizzi M, Birren B and Lander ES (2003) Sequencing and comparison of yeast species to identify genes and regulatory elements. *Nature* **423**, 241–254.
- 20 Barnett DW, Garrison EK, Quinlan AR, Stromberg MP and Marth GT (2011) BamTools: a C++ API and toolkit for analyzing and managing BAM files. *Bioinformatics* **27**, 1691–1692.
- 21 Schulz MH, Zerbino DR, Vingron M and Birney E (2012) Oases: robust *de novo* RNA-seq assembly across the dynamic range of expression levels. *Bioinformatics* **28**, 1086–1092.
- 22 Zerbino DR and Birney E (2008) Velvet: algorithms for *de novo* short read assembly using de Bruijn graphs. *Genome Res* **18**, 821–829.
- 23 Zur H, Ruppin E and Shlomi T (2010) iMAT: an integrative metabolic analysis tool. *Bioinformatics* **26**, 3140–3142.
- 24 Heavner BD, Smallbone K, Barker B, Mendes P and Walker LP (2012) Yeast 5—an expanded reconstruction of the *Saccharomyces cerevisiae* metabolic network. *BMC Syst Biol* **6**, 55.
- 25 Gentleman RC, Carey VJ, Bates DM, Bolstad B, Dettling M, Dudoit S, Ellis B, Gautier L, Ge YC, Gentry J *et al.* (2004) Bioconductor: open software development for computational biology and bioinformatics. *Genome Biol* **5**, R80.
- 26 Anders S and Huber W (2010) Differential expression analysis for sequence count data. *Genome Biol* **11**, R106.
- 27 Mortazavi A, Williams BA, McCue K, Schaeffer L and Wold B (2008) Mapping and quantifying mammalian transcriptomes by RNA-Seq. *Nat Methods* **5**, 621–628.
- 28 Siepel A, Bejerano G, Pedersen JS, Hinrichs AS, Hou MM, Rosenbloom K, Clawson H, Spieth J, Hillier LW, Richards S *et al.* (2005) Evolutionarily conserved elements in vertebrate, insect, worm, and yeast genomes. *Genome Res* **15**, 1034–1050.
- 29 Schraiber JG, Mostovoy Y, Hsu TY and Brem RB (2013) Inferring evolutionary histories of pathway regulation from transcriptional profiling data. *PLoS Comput Biol* **9**, e1003255.
- 30 Heavner BD, Smallbone K, Barker B, Mendes P and Walker LP (2012) Yeast 5 - an expanded reconstruction of the *Saccharomyces cerevisiae* metabolic network. *BMC Syst Biol* **6**, 55.
- 31 Heavner BD, Smallbone K, Price ND and Walker LP (2013) Version 6 of the consensus yeast metabolic network refines biochemical coverage and improves model performance. *Database-Oxford* **2013**, bat059.
- 32 Orth JD, Thiele I and Palsson BO (2010) What is flux balance analysis? *Nat Biotechnol* **28**, 245–248.
- 33 Segre D, Vitkup D and Church GM (2002) Analysis of optimality in natural and perturbed metabolic networks. *Proc Natl Acad Sci USA* **99**, 15112–15117.
- 34 Lun DS, Rockwell G, Guido NJ, Baym M, Kelner JA, Berger B, Galagan JE and Church GM (2009) Large-scale identification of genetic design strategies using local search. *Mol Syst Biol* **5**, 296.
- 35 Becker SA, Feist AM, Mo ML, Hannum G, Palsson BO and Herrgard MJ (2007) Quantitative prediction of cellular metabolism with constraint-based models: the COBRA Toolbox. *Nat Protoc* **2**, 727–738.
- 36 Li C, Jiang W, Ma N, Zhu Y, Dong X, Wang D, Meng X and Xu Y (2014) Bioaccumulation of cadmium by growing *Zygosaccharomyces rouxii* and *Saccharomyces cerevisiae*. *Bioresour Technol* **155**, 116–121.
- 37 Giaever G, Chu AM, Ni L, Connelly C, Riles L, Veronneau S, Dow S, Lucau-Danila A, Anderson K, Andre B *et al.* (2002) Functional profiling of the *Saccharomyces cerevisiae* genome. *Nature* **418**, 387–391.
- 38 Bindea G, Mlecnik B, Hackl H, Charoentong P, Tosolini M, Kirilovsky A, Fridman WH, Pages F, Trajanoski Z and Galon J (2009) ClueGO: a Cytoscape plug-in to decipher functionally grouped gene ontology and pathway annotation networks. *Bioinformatics* **25**, 1091–1093.
- 39 Dotsch A, Klawonn F, Jarek M, Scharfe M, Blocker H and Haussler S (2010) Evolutionary conservation of essential and highly expressed genes in *Pseudomonas aeruginosa*. *BMC Genom* **11**, 234.
- 40 Nei M and Gojobori T (1986) Simple methods for estimating the numbers of synonymous and nonsynonymous nucleotide substitutions. *Mol Biol Evol* **3**, 418–426.
- 41 Tamura K, Peterson D, Peterson N, Stecher G, Nei M and Kumar S (2011) MEGA5: molecular evolutionary genetics analysis using maximum likelihood, evolutionary distance, and maximum parsimony methods. *Mol Biol Evol* **28**, 2731–2739.

- 42 Oberhardt MA, Palsson BO and Papin JA (2009) Applications of genome-scale metabolic reconstructions. *Mol Syst Biol* **5**, 320.
- 43 Nielsen J, Larsson C, van Maris A and Pronk J (2013) Metabolic engineering of yeast for production of fuels and chemicals. *Curr Opin Biotechnol* **24**, 398–404.
- 44 Jerby L, Shlomi T and Ruppin E (2010) Computational reconstruction of tissue-specific metabolic models: application to human liver metabolism. *Mol Syst Biol* **6**, 401.
- 45 Lin Y and Tanaka S (2006) Ethanol fermentation from biomass resources: current state and prospects. *Appl Microbiol Biotechnol* **69**, 627–642.
- 46 Zelezniak A, Pers TH, Soares S, Patti ME and Patil KR (2010) Metabolic network topology reveals transcriptional regulatory signatures of type 2 diabetes. *PLoS Comput Biol* **6**, e1000729.
- 47 Zhang Y, Thiele I, Weekes D, Li ZW, Jaroszewski L, Ginalski K, Deacon AM, Wooley J, Lesley SA, Wilson IA *et al.* (2009) Three-dimensional structural view of the central metabolic network of *thermotoga maritima*. *Science* **325**, 1544–1549.
- 48 Zhao YQ and Huang JF (2011) Reconstruction and analysis of human heart-specific metabolic network based on transcriptome and proteome data. *Biochem Biophys Res Co* **415**, 450–454.
- 49 Lass-Flörl C (2009) The changing face of epidemiology of invasive fungal disease in Europe. *Mycoses* **52**, 197–205.
- 50 Pitman SK, Drew RH and Perfect JR (2011) Addressing current medical needs in invasive fungal infection prevention and treatment with new antifungal agents, strategies and formulations. *Expert Opin Emerg Drugs* **16**, 559–586.
- 51 Butts A and Krysan DJ (2012) Antifungal drug discovery: something old and something new. *PLoS Pathog* **8**, e1002870.
- 52 Chavali AK, D'Auria KM, Hewlett EL, Pearson RD and Papin JA (2012) A metabolic network approach for the identification and prioritization of antimicrobial drug targets. *Trends Microbiol* **20**, 113–123.

## Supporting information

Additional supporting information may be found in the online version of this article at the publisher's web site:

**Fig. S1.** The phastCons tree model for four yeast species.

**Fig. S2.** The Gene Ontology molecular functions enrichment of transcripts *Saccharomyces cerevisiae* not included in the consensus dataset.

**Fig. S3.** The compartmentalization of the consensus metabolic model.

**Fig. S4.** Network simulation of phenotypic characteristics.

**Table S1.** Yeast-specific reactions in consensus metabolic model.

**Text S1.** The consensus metabolic model for four yeast species in Systems Biology Markup Language.